Eye Detection Applying a Probabilistic Algorithm Inspired to the Butterfly Flight

Giuliani Donatella *donatella.giuliani@unibo.it*
School of Economics, Management and Statistics
University of Bologna
Bologna, 40126, Italy

Abstract

Eye state analysis is relevant to detect fatigue and drowsiness when driving, it is therefore essential to ensure safety of people. In this work, we propose an eye detection method applied to color images, recurring to a random exploration performed by multiple research agents simultaneously. The color image is represented in YCbCr color space, because in this space the luminance component is separated by chrominance components. At first, an algorithm is used to recognize the face area in the original image. Afterwards, a normalized EyeMap is generated to distinguish and enhance eye regions in order to make them more evident. For comparison, we performed the procedure on the YCbCr and the Chromaticity Space xy, recurring to a generalized equation. The novelty of this approach is the introduction of the z component of the Chromaticity Space. This choice is justified by its relationship with the Tristimulus Z component, which represents mostly blue wavelengths in turn strictly related to the bluish color of the sclera.The search of ocular areas is conducted through an algorithm that simulates the flight of butterflies. Initially a butterfly gives rise to a random research but, when a foraging zone is discovered, it makes non-random dispersal movements around the food source. Similarly, in the applied algorithm, if a small region containing eyes is detected, even if partially, a more circumscribed research gets started through helicoidal paths around the identified area. In this way, we avoid the arbitrariness of choosing the position and size of any search window.

Keywords: Image Segmentation, Eye Detection, Skin Detector, EyeMap, Nature-inspired Algorithm.

1. INTRODUCTION

Drowsiness and drivers' tiredness have become some of the most important causes of traffic accidents. A large number of unfortunate fatalities could be avoided if drowsiness was detected in time and a security system was activated to prevent the accident. To this aim, researchers have proposed many fatigue detection methods, which can be divided into three types: physiological indicators, vehicle behaviors, and facial analysis, (Kaplan et al., 2015). The first method measures the biological parameters of drivers, such as brain waves, heart rate, muscle tone and temperature (Lin et al.,2005), (Lin et al.,2010). These techniques require physical contact with the driver, so they are intrusive. Consequently, they cannot be used in practice, even though their high level of accuracy. The second type of indicators measures vehicle behaviors such as speed, rotation angle of steering wheel, lateral position, lane departure detection, etc. (Wierwille, 1994). These methods can be implemented non-intrusively, but they depend on type and status of vehicle, the dexterity at the wheel of the driver and the external driving conditions. Furthermore, they need a special equipment, which can be expensive. The third method analyzes the facial expressions of driver, even if it can be less accurate than previous ones, it is non-intrusive and easily implemented. This approach resorts to using indicators such as the percentage of the closing time of the eyelid over a specific time interval, blink frequency, head posture, yawn detection, etc. (Lenskiy et al., 2012), (Saradadevi et al.,2008), (Kim et al.,2020), (Murata et al.,2022). They are non-invasive and essentially come from image processing techniques.

In this work, we propose an eye detection method applied to color image, recurring to a random exploration performed by multiple research agents contemporary. At first, a skin classifier is used to recognize the face area in the original image. To this end, the color image is represented intodifferent color spaces, more precisely RGB, HSV and YCbCr color spaces, in order to compare the efficiency of the skin detector. Afterwards, a normalized EyeMap is generated to distinguish and enhance eye regions in order to make them more evident. The EyeMap was computed using different analytical formulas and representing the original image into two color spaces, the YCbCr and the Chromaticity Space xy, with the aim of doing a comparative analysis. The choice of such color spaces is justified by the fact that in themthe luminance component is separated by chrominance components. The search of ocular areas is carried out by simulating the flight of butterflies.

This paper is organized as follows: firstly introduces the construction of color models for skin and non-skin classes from images; secondly, it illustrates the applied eye detection method; thirdly, it sets out the experimental results; and lastly it concludes with a summary of the results and possible future paths for this research.

2. LITERATURE REVIEW

2.1 History and Background

The variety of techniques proposed for face detection in literature can be grouped in four main categories: 1) template matching-methods, 2) knowledge-based methods, 3) appearance-based methods, 4) invariant features methods (Yang et al., 2002).

1) Template matching methods are based on static or deformable standard patterns, which characterize the shape of face or parts of it such as eyes, nose or mouth contours (Craw et al., 1987). However, these methods are frequently unsatisfying under variations in scale, pose or shape. Consequently, multiresolution, multiscale, sub-templates and active contours are implemented to ensure scale and shape invariance (Leymarie et al., 1993).
2) Knowledge-based methods recur to the knowledge of the shared characteristics of human faces, i.e. two eyes, mouth, nose, two nostrils etc. and their metric and geometrical relationships, such as symmetry, distance between eyes or nostrils, etc. Moreover, if the predefined criteria are too strict, these approaches may give false negative, if not false positive. To overcome these drawbacks, some authors (Yang et al.,1994), (Zhang et al., 2008) suggested a multiresolution approach.
3) Appearance-based methods are derived by statistical analysis of some shareable features between human faces, generally inferred by a set of training images. Most of these methods are framed in a probabilistic context that involves a high computational cost (Rowley et al., 1998), (Sung et al., 1998).
4) Invariant features methods are based on searching structural features, such as eyes, eyebrows, nose, mouth and hairline, which are invariant for pose, viewpoint or lighting conditions.

This work belongs to the appearance-based category. During the last decades, the construction of statistical color models for the detection of face skin was made indeed possible thanks to the huge amount of training datasets currently available (Ban et al., 2014). The color skin characteristics are relatively similar among human beings, consequently the skin and non-skin classes show a high degree of separability, which is the basis of the proposed model of skin detector (Gejgus et al., 2004).

Within the facial analysis methods, the image-based approaches for eye detection are mainly partitioned into four major categories: the shape-based, the model-based, the feature-based and the appearance-based methods (Xie et al.,1994).

Shape-based methods can in turn be divided into fixed shape and deformable shape. Generally, these methods recur to static or deformable template matching, essentially a standard model is

used for searching eyes on the whole image or part of it (Khotari et al., 1996), (Hansen et al, 2010). The reliability of this approach may be compromised by the fact that eye shapes are greatly influenced by observer viewpoint. In this context, to improve the performance of eye recognition, frequently the template matching is accomplished applying a multiple scale analysis. The model-based methods are aimed at face and facial components localization. Even in this case, the use of a multiscale approach or a normalized image representation can enhance the research efficiency. Actually, they are strongly affected by image noise, image scale, face orientation, since the detection of face components makes use of biometric measures between eyes, eyebrows, mouth, nose and nostrils positions, etc. (Huang et al., 2000).

The feature-based methods explore some special characteristics to distinguish human eyes from other facial elements, such as white sclera, dark pupils, circular iris, eye shapes etc. (Zhou et al., 2004)

The appearance-based methods detect eyes based on photometric properties, measuring of light brightness perceived from human eyes. These approaches have proved very effective in human gaze tracking (Jiang et al., 2019), (Hassaballah et al., 2009). In most cases, they need to have available a great amount of training data, due to the variability generated by different illumination conditions, face positions and eye orientations. We can reasonably ascribe the intensity-methods to the appearance-based category given that they are based on evaluation of image intensity as a searching tool.

Alongside the aforementioned approaches, to detect and locate pupil centers Kith V. et al. (2008) applied a hybrid method that combines a feature-based method to detect all possible regions of each left and right eye, and an appearance-based method to filter out all non-eye regions.

The approach for eye detection presented in this paper belongs to the appearance-based group, thus a pre-processing phase is essential since these typologies of eye detection methods are greatly sensitive to illumination variations.

3. RESULTS

3.1 Skin Model

The initial step is to detach face regions from the background to realize an eye detection with a high level of accuracy. For this reason, an initial pre-processing phase is implemented. It consists of transforming the RGB image in HSV (Hue, Saturation, Value) color space. The HSV color space represents any color in the same way in which it is perceived by human eyes: Hue defines the color tone (red,blue etc); Saturation defines the amount of each color (i.e. dark green or pale green); and Value allows to distinguish between a dark or a light color. Consequently, in order to regularize lightness we have applied a Gaussian Filter with $\sigma = 2.0$ only on the Value component. Afterwards, we proceed to label skin and non-skin pixels through a skin detector.

Basically there are three major approaches for skin detection: rule-based, machine learning and hybrid. Generally, machine learning and hybrid approaches outperform the rule-based methods, but require a huge and representative training dataset therefore imply high computational costs. In this paper, we opted for the first class of methods that delimit, through pre-defined rules, the geometric boundaries of the clusters formed by skin pixels in the selected color spaces.

In this context, the regions of skin tone pixels are defined with a straightforward rule, recurring to a specific range of values of color components. We applied a threshold-based algorithm on three different color spaces, more specifically the RGB, HSV and YCbCr spaces, with the purpose of carrying out a comparative analysis aimed at determining the most suitable color space.

The implemented skin classifier performs an image segmentation into two classes, verifying if a skin pixel falls into a defined range of values in the selected color space.

Into the RGB space, the preselected lower and upper limits are [140,85,35] and [255,220,170] respectively.

Into the HSV space the chosen interval has as lower limit [0, 70, 60], instead as upper limit we made the selection [50,150, 255].

For what concerns the YCbCr color space, the human color skin model can be considered independent by the luminance component Y. Practically, it results concentrated in a small region of the Cb-Cr plane, where Cb is the difference between the luminance and the blue component and Cr is the difference between the luminance and the red component. The human skin colors into the Cb-Cr domain [16, 240] x [16, 240] are approximately associated to the rectangular region defined by Cb = [82,124] and Cr = [136,192] (De Dios et al.,2003).

The chosen set of frontal images represent human faces with different expressions, orientations and lighting conditions. We performed face detection by means the aforementioned thresholding technique in the three specified color space. As illustrated in Fig.1, Fig.2, Fig.3, Fig.4, Fig.5,wemay come to the conclusion that the best results were achieved operating on the YCbCr space. After all, the effectiveness of this color space for the detection of skin color is also highlighted in a comparative study carried out by Shaik K.B. et al., (Shaik et al., 2015).Albiol et al. (Albiol et al., 2001) assumed that the efficiency of YCbCr could be due to the compactness of the groupings formed by skin pixels in the Cb-Cr plane. The YCbCr color space was also adopted by Kovac et al. (Kovac et al., 2003), obtaining a true positive rate of about 90%.

Faria R.A.D. et al. (Faria et al.,2018) and Brancati et al. (Brancati et al., 2017) introduced a meaningful improvement on the rule-based skin detection method working in the YCbCr color space. Given that usually skin pixels do not appear isolated, they proposed an extension of the applied rules and suggested taking into account the level of correlation between pixels belonging to the same neighbor.

After being selected the skin mask on YCbCr color space, we executed the morphological operation of region filling on the binary mask, in order to assign the white color to all the pixels belonging to the interior regions.

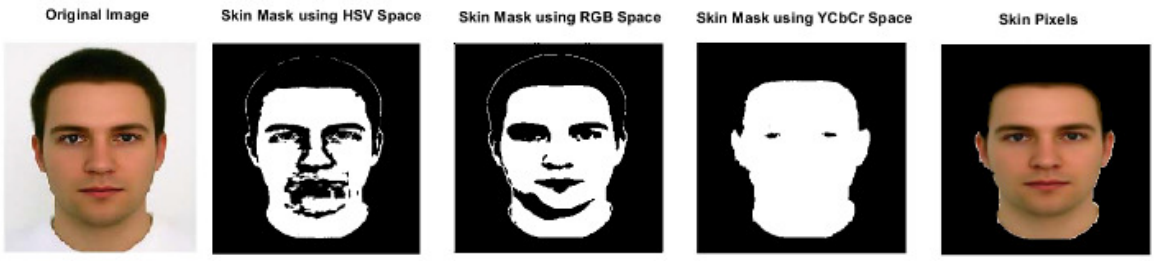

FIGURE 1: Segmentation of skin pixels of the first test image.

FIGURE 2: Segmentation of skin pixels of the second test image.

FIGURE 3: Segmentation of skin pixels of the third test image.

FIGURE 4: Segmentation of skin pixels of the forth test image.

In Fig.5 the background appears rather similar to the skin color, so it was detected as a possible facial region. Actually, as we will show later, this outcome does not compromise the search of eyes.

FIGURE 5: Segmentation of skin pixels of thefifth test image.

3.2 EyeMap In Different Color Spaces

After being segmented the facial features from the composite background, we executed the procedure for eye region detection. Our approach is based on the EyeMap generation that provides a powerful tool for visualizing binocular zones. By representing the image in the YCbCr color space, the localization of eyes is made possible through the measurements of the chroma defined by Cb and Cr. In particular, around the eyes the chrominance components indicate high Cb and low Cr values, whereas eyes, usually, contain both dark and bright pixels in the luma component Y. The EyeMap is generated producing gray intensities that brightens both the eyes and suppresses other facial areas (Hsu et al., 2002), (Kalbkhani et al., 2013). In this work we proposed three different types of EyeMap. The first two were constructed by using the Cb and Cr components and applying the following formulas:

$$\text{EyeMap} = \frac{1}{3}\left(\sqrt{\text{Cb}} - \sqrt{(1-\text{Cr})} + \frac{\text{Cb}}{\text{Cr}}\right) \quad (1)$$

$$\text{EyeMap} = \frac{1}{3}\left(\text{Cb}^2 - \sqrt{(1-\text{Cr})} + \frac{\text{Cb}}{\text{Cr}^2}\right) \quad (2)$$

Therefore, the EyeMaps calculated with Eq. (1) and (2) were normalized, the corresponding outcomes are shown in Fig. 6, Fig. 7, Fig. 8, Fig. 9. As we can observe, the Eyemaps generated by Eq. (2) appear with more uniform and homogeneous gray tones enhancing the lighter ocular

areas. After all, the squaring of Cb in the first term and of Cr in the denominator of the third term increases the contribution due to these two terms. Thereby, the algorithm for researching eyes will result more accurate and efficient if performed with the second type of EyeMap.

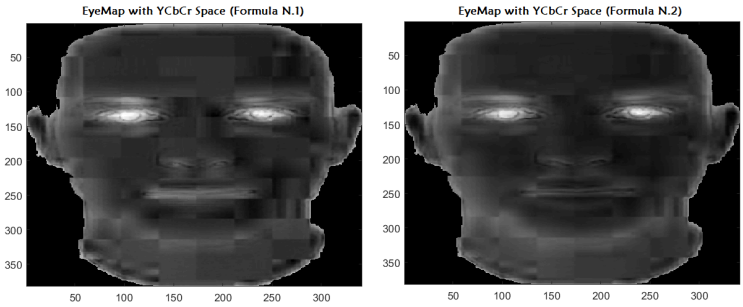

FIGURE 6: EyeMap of image of Fig.1 with formulas (1) and (2).

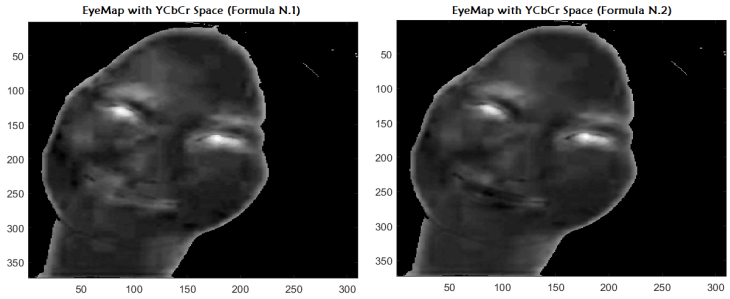

FIGURE 7: EyeMap of image of Fig.2 with formulas (1) and (2).

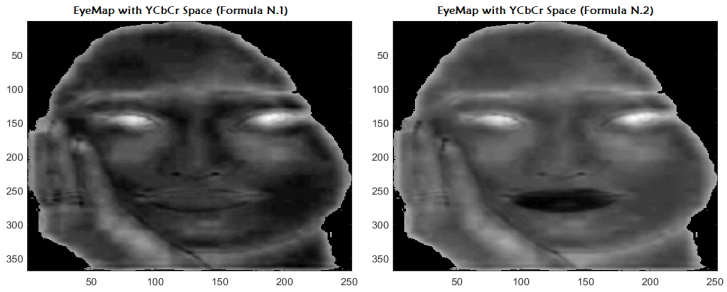

FIGURE 8: EyeMap of image of Fig.3 with formulas (1) and (2).

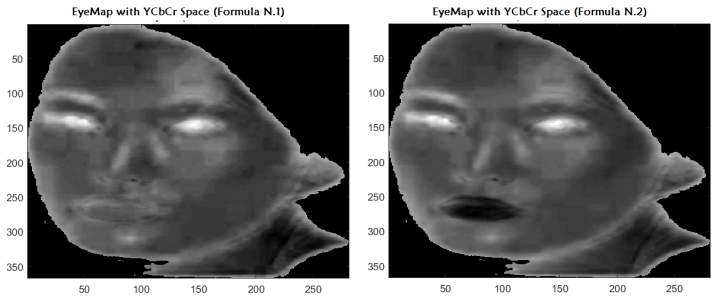

FIGURE 9: EyeMap of image of Fig.4 with formulas (1) and (2).

Moreover, we have generated the EyeMap even using the Chromaticity Space xy with the aim of doing a comparative analysis. The chromaticity coordinates x, y define a point on the 2D

Chromaticity Diagram (Fig. 10a). Chromaticity is a quantitative definition of the quality of a color regardless of its luminance, which consists of two independent parameters x and y, defining the hue and the colorfulness or saturation, respectively. These coordinates are determined from the Tristimulus Values X,Y,Z of the CIE XYZ color space. The human eye has three types of cone cells that are stimulated by different wavelengths of light. The Tristimulus Values X,Y,Z represent the responses of these three types of cones of the human eye with peaks at Long, Medium, and Short wavelengths, see Fig.10b.

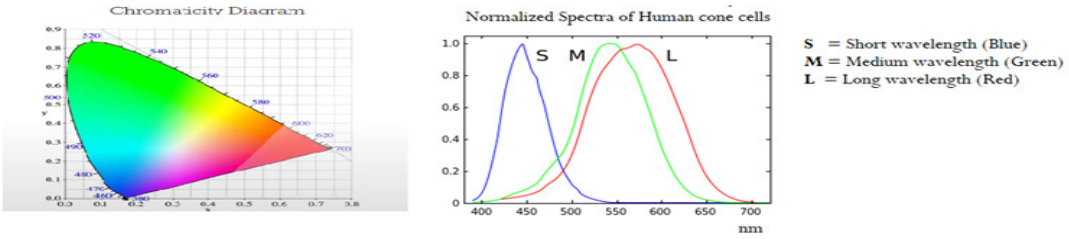

FIGURE 10: 10a) Chromaticity Diagram; 10b) Spectra of human cone cells.

At first, we applied the transformation from the Standard RGB Space (sRGB) to chromaticity XYZ using the following formulas:

$$\begin{pmatrix} X \\ Y \\ Z \end{pmatrix} = M \begin{pmatrix} r_{lin} \\ g_{lin} \\ b_{lin} \end{pmatrix}$$

where

$$M = \begin{pmatrix} 0.4124 & 0.3576 & 0.1805 \\ 0.2126 & 0.7152 & 0.0722 \\ 0.0193 & 0.1192 & 0.9505 \end{pmatrix} \begin{pmatrix} r_{lin} \\ g_{lin} \\ b_{lin} \end{pmatrix} = \begin{pmatrix} \left(\frac{R}{255}\right)^{2.2} \\ \left(\frac{G}{255}\right)^{2.2} \\ \left(\frac{B}{255}\right)^{2.2} \end{pmatrix}$$

where $(r_{lin}, g_{lin}, b_{lin})$ are the RGB linear components, that is to say without the gamma correction $\gamma = 2.2$. After evaluating the Tristimulus Values X,Y,Z, the chromaticity coordinates x, y and z of the Chromaticity space are calculated by:

$$x = \frac{X}{X + Y + Z}$$
$$y = \frac{Y}{X + Y + Z}$$
$$z = \frac{Z}{X + Y + Z}$$

such a definition obviously implies $x + y + z = 1$. Therefore, we generated the EyeMap recurring to the formulas:

$$\text{EyeMap} = \frac{1}{3}\left(z^{\alpha} - \sqrt{(1 - \text{x})} + \left(\frac{z}{x}\right)^{\beta}\right) \qquad (3)$$

with $\alpha, \beta > 1$ and $z = 1 - x - y$.

The introduction of z component in Eq. (3) is due to its relationship with the Tristimulus Z component, which represents mostly blue wavelengths. In fact, in non-pathological conditions, the sclera takes on a bluish color, since being not very thick, it reveals the underlying uvea, rich in blood vessels.

Actually, we suggest to observe the first four rows of the colored squared table in Fig.11, thatrepresent four different colors. More precisely, in the first row three different yellow colors are displayed with the same Hue = 40, in the second row three different red colors with Hue = 0, etc. Synthetically, the pre-selected colors are characterized by different Hue component but equal Saturation and Value coordinates, as shown more explicitly in Table 1.

In the last row of the colored squared table, three different light colors are displayed, then with different values of the hue components: a light yellow (H=40, S=240, V=230), a light blue (H=160, S=240, V=230), a light red (H=0, S=240, V=230). Analyzing the Tristimulus components of the selected colors, we note that only the colors with a high level of brightness are not obscured in the Z component, except for the pure blue color (the second color of the fourth row), which, in any case, cannot be the color of the sclera. In conclusion, the choice of the z component seems to be suitable for accomplishing the search for the brightest parts of the face, namely the eyes.

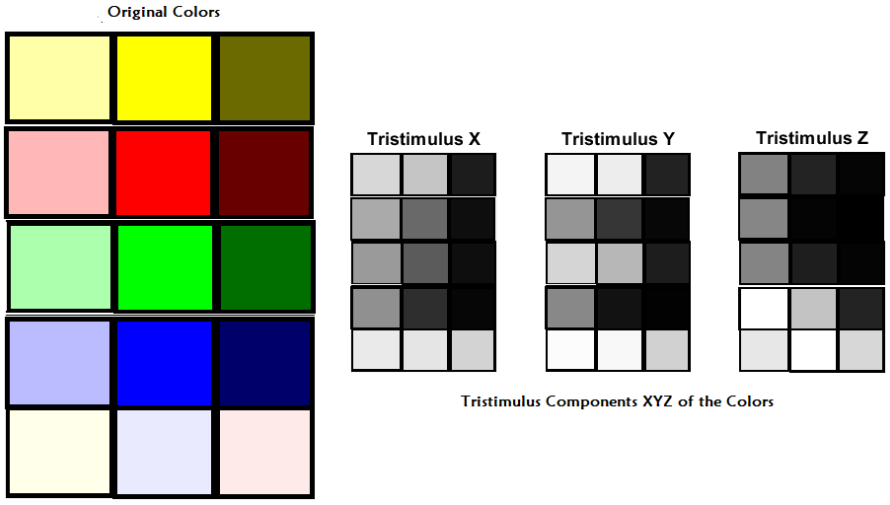

FIGURE 11: Original colors and their corresponding XYZ components

	HSV components of rows 1,2,3,4 of Fig. 11		
YellowY	H= 40 S= 240 V= 120	H= 40 S= 240 V= 200	H= 40 S= 240 V= 50
RedR	H= 0 S= 240 V= 120	H= 0 S= 240 V= 200	H= 0 S= 240 V= 50
GreenG	H= 80 S= 240 V= 120	H= 80 S= 240 V= 200	H= 80 S= 240 V= 50
BlueB	H= 160 S= 240 V= 120	H= 160 S= 240 V= 200	H= 160 S= 240 V= 50

TABLE 1: HSV components of rows 1,2,3,4 of Fig. 11.

Even in the Chromaticity Space xy, the EyeMaps present a remarkable contrast between the orbital areas and the remaining parts of the face. In this context, the facial lineaments are more distinguishable, especially lips and nose (Fig.12).

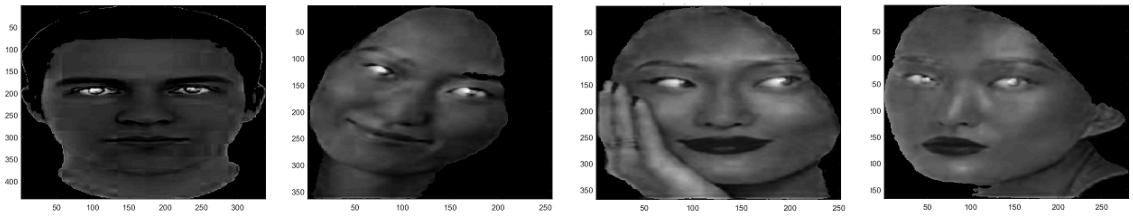

FIGURE 12: EyeMaps with $\alpha = 3$ and $\beta = 2$.

The EyeMaps brighten both the eyes with more and more evidence obscuring other facial features, if we choose the parameter values $\alpha = 4$ and $\beta = 3$ in Eq. 3 or $\alpha = 4$ and $\beta = 4$, as shown in Fig.13 and Fig.14. Therefore, the proposed formulas of Eq. (3) represents a valid alternative to create the EyeMap in the Chromaticity Space xy rather than YCbCr color space.

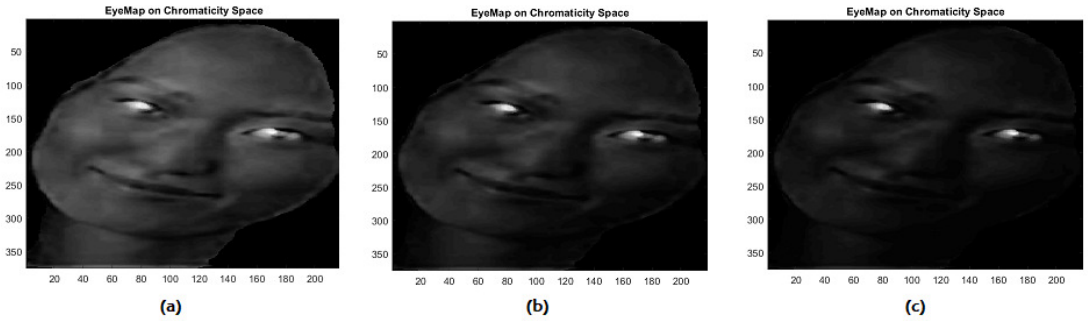

FIGURE 13: EyeMaps of image of Fig.2 with (a) $\alpha = 3$ and $\beta = 2$; (b) $\alpha = 4$ and $\beta = 3$; (c) $\alpha = 4$ and $\beta = 4$.

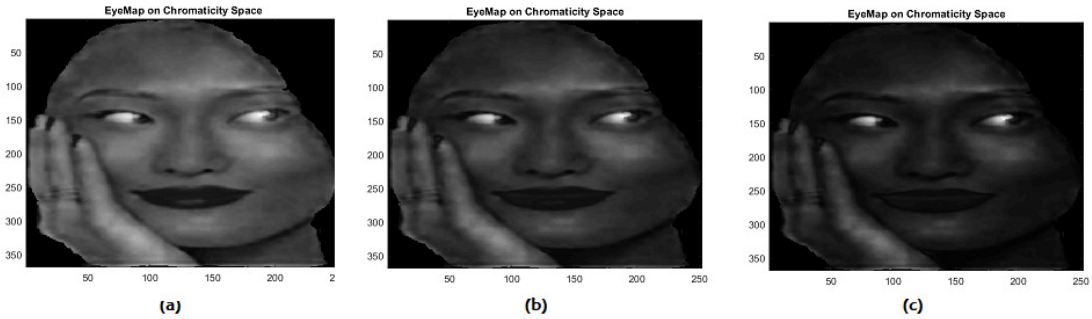

FIGURE 14: EyeMaps of image of Fig.3 with (a) $\alpha = 3$ and $\beta = 2$; (b) $\alpha = 4$ and $\beta = 3$; (c) $\alpha = 4$ and $\beta = 4$.

3.3 Probabilistic Algorithm for Eye Detection

After obtaining the EyeMap, we performed a probabilistic and nature-inspired algorithm based on the butterfly flight pattern.

Butterfly flights were categorized into three different styles (A, B and C) which significantly differ in flight distance, ground speed and straightness (Cant et al., 2005), (Conradt et al., 2000).

The first style (type A) is essentially characterized by linear flight paths. It is carried out in absence of nectar rich plants, hence these zones are overflown without stopping to forage. The second style B is nonlinear and slower, with looped sections of flight involving foraging activity. Such loops allow the butterflies to return to the areas of forage with slower velocity but moving more zigzagging and forming loops, circle or spiral paths, with the aim to better explore the foraging regions. Finally, during the style C of the flight, the butterflies spend the majority of time

motionless on the grass, the tracks have low straightness values and the lowest mean ground speed.

In this work, we were inspired by the butterfly research pattern to develop and implement a probabilistic algorithm, which is a procedure where the result is obtained depending on chance, but without compromising the validity of the final solution. The choice of a heuristic approach is justified by the random positioning of the ocular areas in the EyeMap. Furthermore, since the eye areas are the only regions essentially visible on it, a localized search is more appropriate and able to reduce computational costs. Although a unique solution does not exist, this process still guarantees to complete effectively and efficiently the detection of eyes.

This non-deterministic approach allows us to discover possible solutions by exploring a search space, the EyeMap, employing multiple research agents, the butterflies, randomly generated, in order to find possible solutions. The algorithm starts moving 50 butterflies around the gray image in casual directions following rectilinear movements of type A. To each search agent is associated a square window of 15x15 pixels. In our simulating modelof butterfly flight, these windows represent foraging areas. If the sum of intensities of the gray-levels of the pixels belongingto a given window is greater than the 60% of the maximum level, they are identified as possible eye-pixels. When a search agent detects an area with possible eye-pixels, starts a local search along a helicoidal tracks, following nonlinear paths of type B. The search for localizing the brightest regions for eye candidates stops when all pixels have been investigated. After having detected the eyes, we then automatically identified the rectangular area around them, defining the principal axis through the minimumsquare method.

To elaborate the test image of Fig.1, we made the selection of the Eyemap generated in the YCbCr color space applying Eq. (2) rather than Eq.(1). As can be seen by analyzing Fig. 6, the head boundaries of the young man are of light gray, consequently the search of ocular areas could be compromised. Then the search activity of the random agents is carried out forming spiral paths (Fig.15) because the associated windows have registered an intensity gray level greater than the threshold value. Fig.16 shows the final outcomes of the eye detection process extracted by the EyeMap (Fig.15a) and superimposed on the original color image (Fig16b).

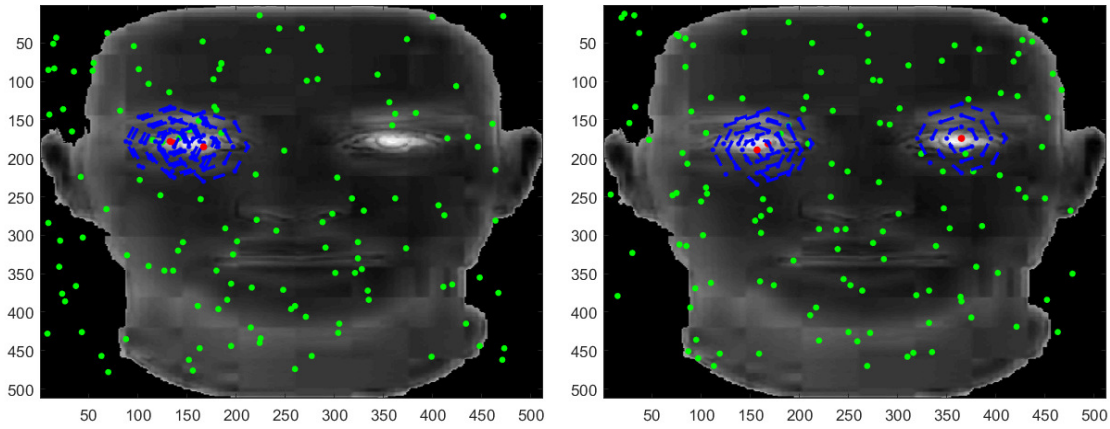

FIGURE 15: Search of ocular areas simulating the butterfly non-linear flights (style B).

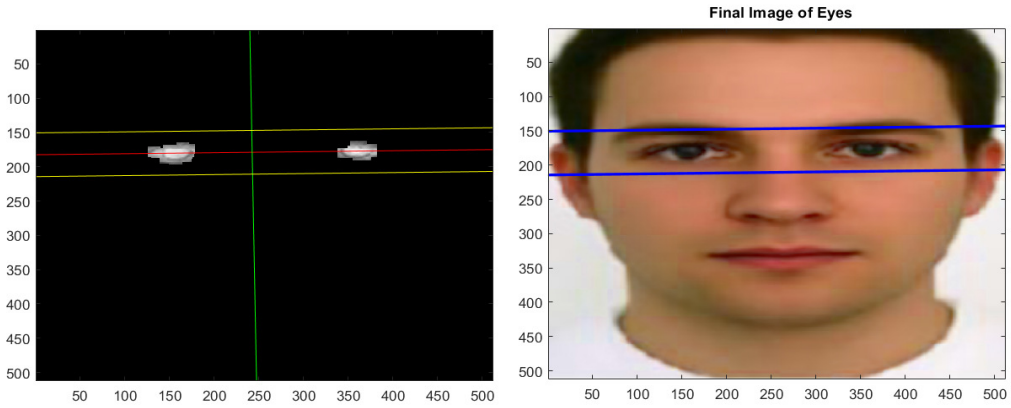

FIGURE 16: 16a) Ocular areas extracted by EyeMap in YCbCr; 16b) Ocular areas on the original image.

To perform eye detection with the test image of Fig.2, we opted for the EyeMap created in the Chromaticity Space xy using Eq. (3) with α=4 and β=4. The helicoidal paths superimposed on the EyeMap are shown in Fig.17. The Fig.18 displays the rectangle that delimits the eye region on both the EyeMap and the original image, respectively. Even in this case the algorithm worked efficiently despite the oblong and almond-shaped eyes and the reclined position of the head.

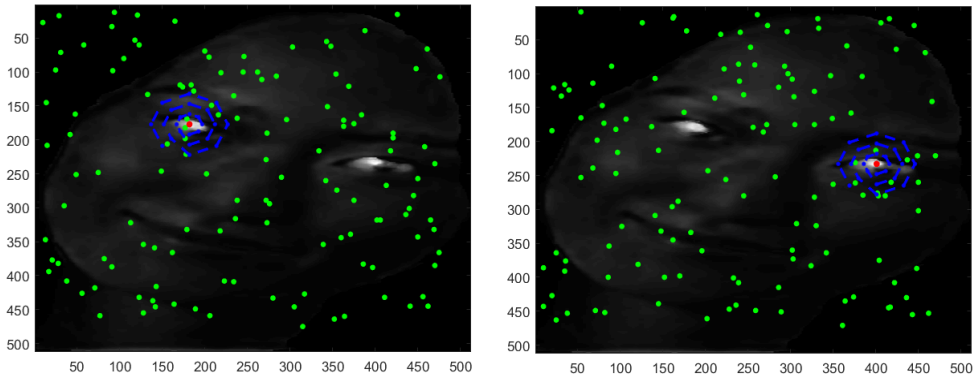

FIGURE 17: Search of ocular areas simulating the butterfly non-linear flights (style B).

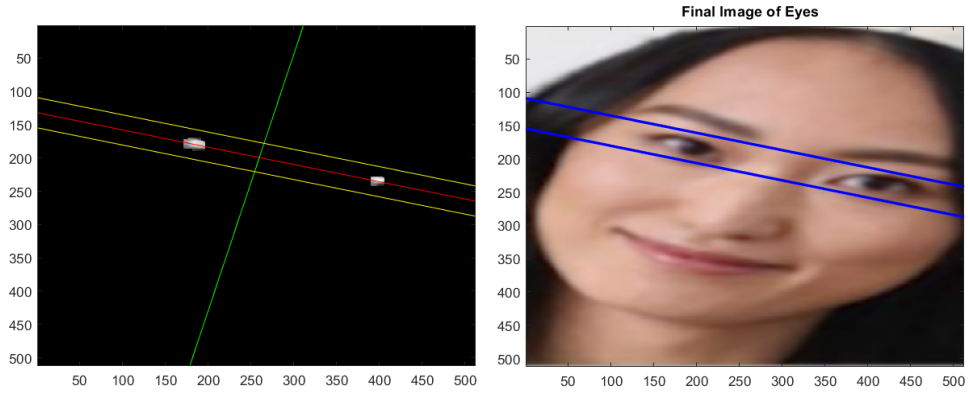

FIGURE 18: 18a) Eye region extracted by EyeMap in Chromaticity space; 18b) Ocular areas on the original image.

Hereinafter, we propose another application to the image of Fig.3 with this eye detection method. At first, the EyeMap, shown in Fig. 19a, is generated recurring to Eq. (2). In this context, the facial features are more evident and there are some fairly clear areas that could compromise the search process such as, for example, parts of the hand and throat. Anyway, the local search for eye detection is carried out successfully.

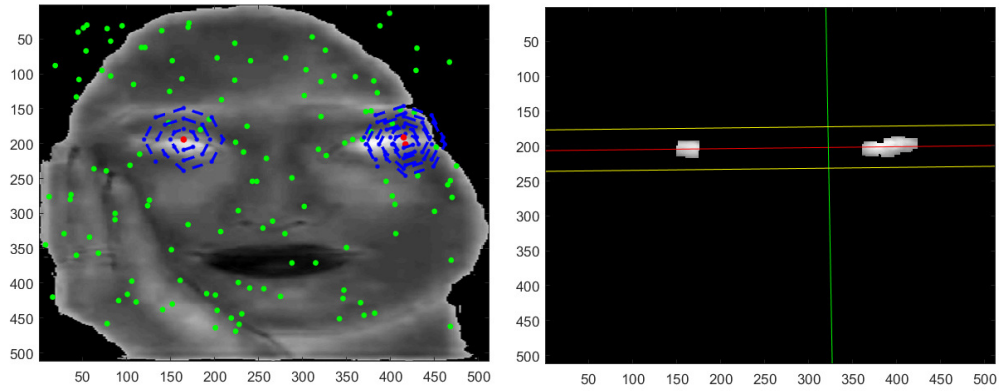

FIGURE 19:19a) Search of ocular areas; 19b) Eye region extracted by the EyeMap in YCbCr space.

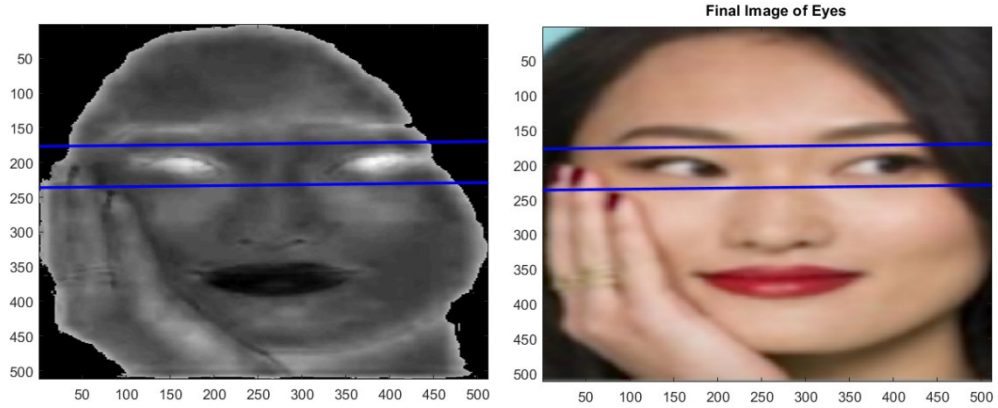

FIGURE 20:20a) Ocular areas with EyeMap in YCbCr; 20b) Ocular areas on the original image.

Secondly, the eye search was performed using the EyeMap (Fig. 21a) produced by Eq. (3) with α=4 and β=4.In this case, the ocular sclera stand out significantly against the rest of the face. Therefore, the region around the eyes is narrower and more defined.

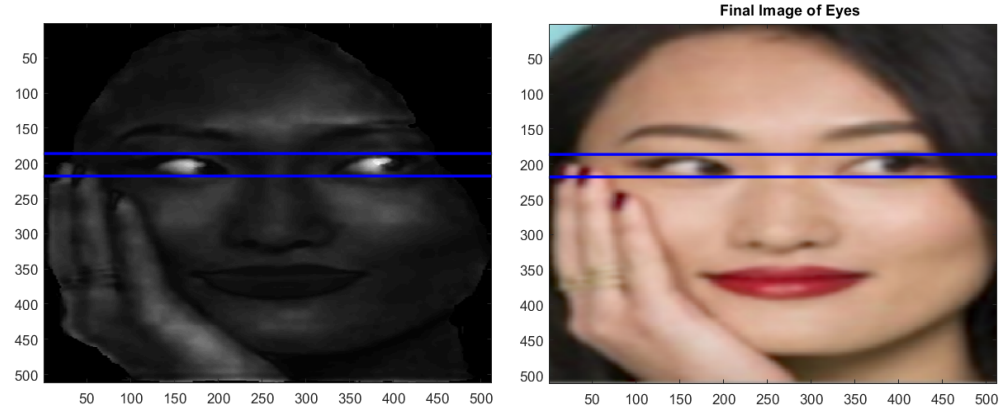

FIGURE 21:21a) Ocular areas with EyeMap in YCbCr; 21b) Ocular areas on the original image.

Although in the image represented in Fig. 5 the background appears rather similar to the skin color, the search of eye regions gives rise to satisfying results, demonstrating the robustness and reliability of this approach, enhanced by the application of a local research (Fig.22).

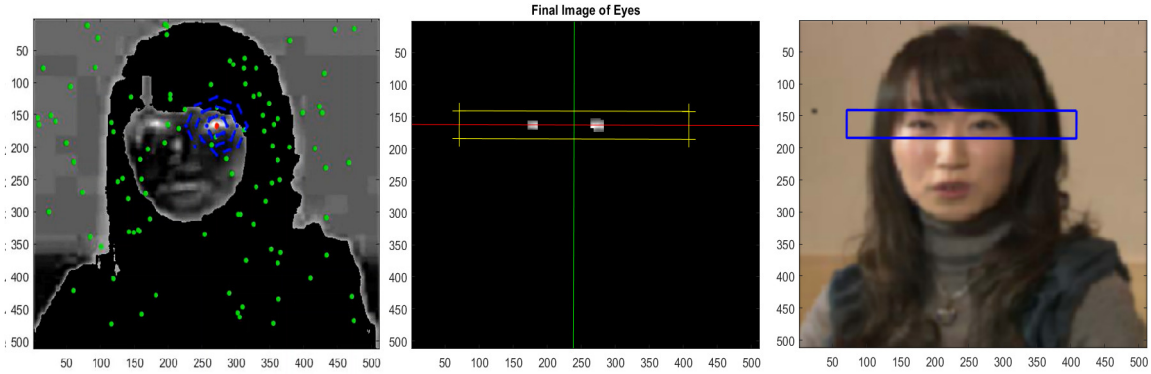

FIGURE 22:22a) Search of ocular areas;22b) Ocular areas extracted by the EyeMap in the YCbCr; 22c) Ocular areas on the original image.

4. CONCLUSIONS

The first part of this work is focused on a comparative analysis of the use of different color spaces in the generation of a skin detector. The experimental results clearly show that if the skin masks are generated on the YCbCr color space, the outcomes significantly improve. In the second part of the paper, we exposed our approach of eye detection that is based on EyeMap generation, a powerful tool for visualizing binocular zones. Even in this case, we brought out different EyeMaps employing two distinct color spaces, the YCbCr and the Chromaticity color spaces, and applying different analytical formulas. The results demonstrate that the proposed use of the Chromaticity Space xy rather than YCbCr color space represents a valid alternative to create the EyeMap, primarily because the contrast between the ocular areas and the remaining face features is sharper.

In order to enhance the detection of the eye region, in the present work we investigated also the Chromaticity Space xy recurring to a more general equation. Our approach is only partially heuristic since the choice to introduce the z component in Eq. (3) is justified by its relationship with the Tristimulus Z component, which represents mostly blue wavelengths. It is rather evident that this fact is closely related to the bluish color of the sclera.

Moreover, in this proposed eye detection method, we suggested considering a probabilistic algorithm that simulates the butterfly behavior, which has demonstrated to be a suitable algorithm for searching ocular regions. Indeed, during the random exploration for food sources, butterfly flights give rise to paths forming loops, circular or spiral trajectories around regions of interest.By simulating such movements, our algorithm has the advantage of activating a local search, which proved to be a more effective alternative than a regular and systematic global search.

However, this method has not been tested with people wearing glasses that may reflect light in an irregular way, which could be more difficult to control.

5. REFERENCES

Albiol, A., Torres, L., &Delp, E. (2001). Optimum color spaces for skin detection, *Proceedings of the International Conference on Image Processing (ICIP)*, 122-124.

Ban,Y., Kim, S. K., Kim, S., Toh, K.A., &Sangyoun, S. (2014). Face detection based on color skin likehood, *Pattern Recognition*, 47, 1573-1585.

Brancati, N., De Pietro, G., Frucci, M., & Gallo, L.(2017). Human skin detection through correlation rules between the YCb and YCr subspaces based on dynamic color clustering, *Computer Vision and Image Understanding*, 155, 33–42.

Cant, E.T., Smith, A.D., Reynolds, D.R.,& Osborne, J.L. (2005). Tracking butterfly flight paths across the landscape with harmonic radar, *Proceedings of the Royal Society B: Biological Sciences*, 272, 785-790.

Conradt, L., Bodsworth, E. J., Roper, T. J., &Thomas,C. D. (2000). Non-random dispersal in the butterfly Maniola jurtina: implications for metapopulation models, *Proceedings of the Royal Society B: Biological Sciences*, 267, 1505-1510.

Craw, I., Ellis, H.,& Lishman, J.R.(1987). Automatic extraction of face-features, *Pattern Recognition Lectures,* 5, 183-187.

De Dios, J.J., &Garcia, N. (2003). Face detection based on a new color space YCgCr, *Proceedings 2003 International Conference on Image Processing*, 14-17.

Faria, R.A.D., & Hirata R. jr. (2018). Combined Correlation Rules to Detect Skin based on Dynamic Color Clustering. *Proceedings of International Conference on Computer Vision Theory and Applications*, 5.

Gejgus, P., Placek, J., &Sperka, M. (2004). Skin color segmentation method based on mixture of Gaussians and its application in learning system for finger alphabet, *International Conference on Computer Systems and Technologies (CompSysTech)*.

Hansen, D., &Ji,Q. (2010). In the Eye of the Beholder: A Survey of Models for Eyes and Gaze, *IEEE Transactions on Pattern Analysis and Machine Intelligence*.

Hassaballah, M., &Ido, S. (2009). Eye detection using intensity and appearance information, *IAPR Conf. on Machine Vision Application*.

Hsu, R. L., Abdel-Mottaleb,M.,& Jain, A.K. (2002). Face detection in color images, *IEEE Transactions on Pattern Analysis and Machine Intelligence*, 24 (5), 696-706.

Huang, W.,& Mariani R. (2000). Face detection and precise eyes location, *Proc. Int. Conf Pattern Recognition*, 722-727.

Jiang, J., Zhou, X., Chan, S., &Chen, S. (2019). Appearance-based gaze tracking: a brief review,*Int. Conf. on Intelligent Robotics and Applications (ICIRA 2019)*, 229-240.

Kalbkhani, H., Shayesteh,M.G., &Mousavi, S.M. (2013). Efficient algorithms for detection of face, eye and eye state, *IET Computer Vision*, 7 (3),184-200.

Kaplan. S., Guvensan, M. A., Yavuz, A. G., & Karalurt, Y. (2015). Driver Behavior Analysis for Safe Driving: A Survey, *IEEE Transactions on Intelligent Transportation Systems,*16 (6), 3017-3032.

Kim, S., Wisanggeni, I., Ros, R., Hussein, R. (2020). Detecting fatigue driving through PERCLOS: a review, *International Journal of Image Processing (IJIP),* 14 (1).

Kith, V., El-Sharkway, M., Bergeson-Dana, T., El Ramly,S. & Elnoubi,S.(2008). A feature and appearance based method for eye detection on gray intensity face images, *Int. Conf. Computer Engineering and Systems*.

Kothari, R.,& Mitchell, J.L. (1996). Detection of eye locations in unconstrained visual images, *Proceedings International Conference on Image Processing*, 3, 519–522.

Kovac, J., Peer, P., & Solina, F. (2003). Human skin color clustering for face detection, *Proceedings IEEE region 8 EUROCON 2003. Computer as a Tool,* 2.

Lenskiy, A., & Lee J. S. (2012). Driver's eye blinking detection using novel color and texture segmentation algorithms, *International Journal of Control, Automation and Systems*, 10, (2), 317–327.

Leymarie, F.& Levine, M. D. (1993). Tracking deformable objects in the plan using an active contour model, *IEEE Transactions on Pattern Analysis and Machine Intelligence*,15 (6), 617-634.

Li, M.Z., Cheng, Z., & Fang, J. F.(2010). An EEG-based method for detecting drowsy driving state, *Proceedings of 7th International Conference on Fuzzy Systems and Knowledge Discovery*, 2164-2167.

Lin, C. T., Chang, C.,J., Lin, B. S., Hung,S. H., Chao, C.F. (2010). A real-time wireless brain–computer interface system for drowsiness detection, *IEEE Transactions. Biomedical Circuits Systems*, 4 (4), 214–222.

Lin,C. T., Wu, R. C.,Liang, S. F., Chao, W. H., Chen, Y. J., & Jung, T.P. (2005). EEG-based drowsiness estimation for safety driving using independent component analysis*, IEEE Trans. Circuits Systems*, 52, (12), 2726–2738.

Murata, A., Doi, T., & Karwowski, W. (2022). Sensitivity of PERCLOS70 to drowsiness level: effectiveness of PERCLOS70 to prevent crashes caused by drowsiness*. IEEE Access*, 10, 70806-70814.

Rowley, H., Baluja, S.& Kanade, T.(1998). Neural network based-face detection, *IEEE Transactions on Pattern Analysis and Machine Intelligence*, 20 (1), 23-38.

Saradadevi, M., & Bajaj, P. (2008). Driver fatigue detection using mouth and yawning analysis, *International Journal of Computer Science and Network Security*, 8, (6), 183–188.

Shaik, K.B., Ganesan, P., Kalist, V., Sathish, B.S. & Merlin, M.J. (2015). Comparative Study of SkinColor Detection and Segmentation in HSV and YCbCr Color Space, *Procedia Computer Science*,57, 41-48.

Sung, K.K.&Poggio, T. (1998). Example-based learning for view-based human face detection, *IEEE Transactions on Pattern Analysis and Machine Intelligence*, 20 (1), 39-51.

Wierwille, W., Ellsworth, L., Wreggit,S., Fairbanks, R., & Kirn, C. (1994). Research on vehicle based driver status/performance monitoring: Development, validation, and refinement of algorithms for detection of driver drowsiness, *National Highway Traffic Safety Administration, Washington,DC, USA, Final Report. DOT HS 808 247*.

Xie, X.,Sudhakar, R.& Zhuang, H. (1994). On improving eye feature extraction using deformable templates, *Pattern Recognition*, 27 (6), 791-799.

Yang, M.H., Kriegman, D. J.&Ahuja, N. (2002). Detecting faces in images: a survey, *IEEE Transactions on Pattern Analysis and Machine Intelligence*, 24 (1), 34-58.

Yang, G. & Huang, T.S. (1994). Human face detection on complex background, *Pattern Recognition*, 27, 53-63.

Zhang, J., Liu ,Y. & Ha, S. W. (2008). A novel approach of face detection based on skin color segmentation and PCA, *The 9th International Conference for Young Computer Scientists IEEE*.

Zhou, Z. &Geng, X.(2004). Projection function for eye detection, *Pattern Recognition*, 37 (5), 1049-1056.